

## Surface Free Energy and Dynamic Wettability of Differently Machined Poplar Woods

Zhiyong Qin, Qiang Gao,\* Shifeng Zhang,\* and Jianzhang Li\*

The surface free energy and dynamic wettability of wood are important to the performance of its adhesive bonding strength. In this work, the surface free energy of poplar wood samples machined with different processes were calculated by the OWRK (geometric mean) and vOCG (acid-base) methods, and the dynamic wettability of adhesives on wood samples was studied using the S-D wetting model. The results indicate that the contact angles of reference liquids on rotary wood samples were greater than those on planed or sawn wood, and the rotary wood samples were more hydrophobic. The effect of surface roughness on contact angle was insignificant compared with surface structure morphology. The total surface free energy was almost the same for the planed and sawn wood, as calculated by the OWRK and vOCG methods, and the surface free energy of rotary wood samples was lower than that of planed or sawn wood samples. The initial and equilibrium contact angle increased as the viscosity of adhesive increased for all the wood samples, and the contact angles of rotary wood samples were greater than those of planed or sawn wood; however, the K-value was lower. The wettability of the loose side was higher than that of the tight side. Contact angles decreased when surface free energy increased, while the K-value increased.

*Keywords:* Machined process; Contact angle; Surface free energy; Penetration; Relationship

*Contact information:* MOE Key Laboratory of Wooden Material Science and Application, Beijing Forestry University, Beijing 100083, China;

\* *Corresponding authors:* gao200482@163.com; hnzsf142@126.com; lijianzhang126@126.com

### INTRODUCTION

Wettability refers to how easily and efficiently a liquid spreads over a solid surface (Baldan 2012). The wettability of wood is an important parameter that provides a series of information on the interaction between the wood surface and liquids (such as water, coating, and adhesives) (Gray 1962; Elbez 1978; Gardner *et al.* 1991; Gindl *et al.* 2004; Rathke and Sinn 2013), which also has a significant influence on the bonding strength of wood composites. Adequate wetting of the wood surface by an aqueous resin solution is a fundamental requirement for a generation of strong adhesive joints (Hse 1972; Jennings *et al.* 2005).

The surface free energy of wood, similar to wettability, is a useful parameter that has often been correlated with the biological interactions of wood. Surface free energy can be calculated by many methods based on the contact angle of liquids on wood (Gindl *et al.* 2001a). Recently, as well as in the past, much research has been undertaken examining differences in wood surface free energy in relation to the properties of porosity and anisotropy. It was found that the species, surface roughness, pH value, and aging time all influenced surface free energy (Cao *et al.* 2005, Gindl *et al.* 2001b, Little *et*

al. 2013, Mohammed-Ziegler *et al.* 2004). Gardner *et al.* studied the dynamic wetting behavior of different wood species using the dynamic contact angle method and studied and compared the methods for calculating surface free energy as well (Gardner *et al.* 1991; Wålinder and Gardner 2002). Gindl *et al.* (2004) determined that the effect of aging time on surface free energy is significant using the contact angle measurements combined with X-ray photoelectron spectroscopy. They also concluded that the acidity of wood compared with surface energy components is a good relative measure for the classical acidity and pH value between different wood species. Vázquez *et al.* (2003, 2011) investigated the effect of veneer side wettability on the bonding quality of *Eucalyptus globulus* plywood prepared using tannin–phenol–formaldehyde adhesive, as well as the surface characterization of rotary-peeled *Eucalyptus* veneers, by confocal laser scanning microscopy.

When a liquid wets wood, three effects can be observed: 1) the formation of an interface between the wood surface and the liquid drop, 2) the spreading of the drop on the wood, and 3) the penetration of the liquid into the wood. Wetting of wood by a liquid is a complex process involving a series of physicochemical processes. Therefore, studying the wetting process may be more meaningful than studying only the initial equilibrium contact angle (Shi and Gardner 2001). There are also many factors (such as surface tension phenomena and viscosity of liquids, wood aging, drying processing, and defects) that influence penetration (Huang *et al.* 2012). Contact angle measurements with a sessile drop method represent a direct method for evaluating the wetting process.

The different processes by which wood is machined may influence the structure, morphology, and chemical composition of the wood surface, which cause the different wettability of liquids on wood. The aim of this work was to determine the influence of different machined processes (planing, dis-sawing, and rotary cutting) for poplar wood surfaces on its wettability. The surface free energy was calculated using the OWRK and vOCG methods. The penetration of phenol formaldehyde adhesives into wood was evaluated using the S-D model, and the relationship between the surface free energy and dynamic wettability was also discussed.

## EXPERIMENTAL

### Materials and Methods

Fast-growing poplar was chosen as the model species because it is widely used in the Chinese wood industry for the preparation of wood panel and furniture (Han *et al.* 2009, Hua and Jin 2006). All of the samples were obtained from a local wood product manufacturer (Hebei, Wen'an Country) and machined by planing, dis-sawing, or rotary cutting (boiling at 80 °C first and then cutting with a rotary cutter at a speed of 32 mm/s) in the laboratory, then placed in air conditioning for seven days before use in the experiment. The average age of wood was 30 years old. They each had final dimensions of 100 mm × 25 mm × 3 mm (length × width × thickness).

In this study, contact angle measurements were tested using a series of three liquids: distilled water, formamide, and diiodomethane. All liquids were of HPLC grade and purchased from Tianjin Chemistry Company. The specifications of their surface tension and components are shown in Table 1 (Van Oss *et al.* 1990).

**Table 1.** Surface Tension and Components of the Test Liquids

Type of Liquid Reference	Surface Free Energy (mJ/m <sup>2</sup> )				
	$\gamma_L$	$\gamma_L^{LW} (\gamma_L^d)$	$\gamma_L^{AB} (\gamma_L^p)$	$\gamma_L^+$	$\gamma_L^-$
Distilled Water	72.8	21.8	51.0	25.5	25.5
Formamide	58.0	39.0	19.0	2.28	39.6
Diiodomethane	50.8	50.8	0	0	0

Phenol formaldehyde (PF) adhesives were chosen to investigate the dynamic wettability of adhesive on wood. PF adhesives with formaldehyde/phenol (F:P) molar ratios of 2.25 were formed in the laboratory. The mixture of phenol (98%), catalyst (sodium hydroxide solution 40%), and formaldehyde aqueous solution (37%) was added into the reactor and stirred uniformly, heated to a temperature of 90 °C, maintained at this temperature for 50 min, then cooled to 80 °C. The second part of the formaldehyde aqueous solution and catalyst were then added into the reactor, heated, and maintained at 90 °C for 30 min. Adhesives with different viscosities were collected every 20 min during the process of reaction and named A1, A2, or A3, according to the sequence of collection. The fundamental properties of the adhesives are listed in Table 2.

**Table 2.** Specifications of the PF Adhesives

Sample	Viscosity (mPa.s)	Surface Free Energy* (mJ/m <sup>2</sup> )	Density g/cm <sup>3</sup>	pH Value	Solid Content (%)
A1	53.7	66.87	1.19–1.21	11.8–12.0	44.37–44.50
A3	102.6	67.79			
A5	189.9	68.23			

\* The surface free energy of the adhesive was characterized using the pendant drop method.

### Image Analysis

Images of the surfaces of machined wood samples parallel to the grain direction with 100× magnification were obtained using scanning electron microscopy. An S-3400N (HITACHI, Japan) scanning electron microscope (SEM) operating at a 10-kV acceleration voltage was used to visualize the surfaces. Prior to imaging, samples were coated with gold–palladium in a sputter coater (E-1010, HITACHI, Japan).

### Surface Roughness Test

According to DIN4768, the roughness parameters of the arithmetic mean of the deviations absolute values of the mean line profile (Ra) were measured using a Surtronic 3+ Roughness tester (Taylor/Hobson Company, England) with a 2-μm diamond stylus tip radius. All measurement results were processed using a digital Gaussian filter. Eight to ten wood samples were used for roughness measurement, and the error of unevenness did not exceed ±10%.

### Contact Angle Measurement

Contact angle measurements on the surfaces of samples parallel to the grain were performed with an optical contact angles apparatus (OCA 20 DataPhysics Instruments GmbH, Filderstadt, Germany) equipped with a video measuring system with a high-resolution CCD camera and a high-performance digitizing adapter that enables instantaneous and frequency registration. SCA 20 software (DataPhysics Instruments

GmbH, Filderstadt, Germany) was used for data acquisition. Sessile Droplets (3  $\mu\text{L}$ , measured with a microsyringe) of liquids (1.5  $\mu\text{L}$  for diiodomethane) were placed on the wood surface, the right and left angles of the drops on the surface were collected at intervals of 0.1 s for a total duration of 80 s, and the average of the angles was calculated for the calculation of surface free energy. For the PF adhesives, the drop volume was 5  $\mu\text{L}$  at an interval of 1 s during the first 10 s and an interval of 10 s for a duration of 80 s. However, it should be mentioned that it is difficult to create an exact volume because of the viscosity of the adhesives.

Three drops per sample were captured for all three liquids and adhesives, four samples were used per liquid, and 12 measurements of contact angle were obtained.

### Determination of Surface Free Energy Components

Many methods have been used to calculate the surface free energy of wood, including the Zisman approach, the equation of state, the harmonic mean equation, the geometric mean equation, and the acid-base approach. The acid-base approach is considered to be the most effective method for calculating the surface free energy of wood composites in many studies because it provides the greatest accuracy in calculating wood composites surface tension components (Gardner 1996; Gindl *et al.* 2001a; Wålinder and Gardner 2002).

In this work, the geometric mean equation and the acid-base approach based on Young's equation  $\gamma_s = \gamma_L \cos\theta + \gamma_{SL}$  were used to evaluate the surface free energy of wood, where  $\gamma_s$  is the surface tension of solid,  $\gamma_L$  is the surface tension of liquid,  $\gamma_{SL}$  is the surface tension of the solid-liquid interface, and  $\theta$  is the contact angle between a solid (S) and a liquid (L).

The geometric mean approach is also known as the OWRK method after its originators Owens, Wendt, Rabel, and Kaelble (Owens and Wendt 1969) and is an extension of Fowkes' models in that the polar (hydrogen bonding) term is also considered. In this approach, the total surface free energy ( $\gamma$ ) is divided into dispersed ( $\gamma^d$ ) and polar ( $\gamma^p$ ) components, the geometric mean to combine the polar and dispersive components together as shown in Eq. 1.

$$\gamma_{SL} = \gamma_s + \gamma_L - 2\sqrt{\gamma_s^d \gamma_L^d} - 2\sqrt{\gamma_s^p \gamma_L^p} \quad (1)$$

Combining Eq. (1) with Young's equation generates the following OWRK method Eq. 2:

$$\gamma_L(1 + \cos\theta) = 2\sqrt{\gamma_s^d \gamma_L^d} + 2\sqrt{\gamma_s^p \gamma_L^p} \quad (2)$$

Because of the presence of the polar term, the minimum number of liquids required to calculate the solid surface components is two of known surface tension.

The acid-base theory has received significant support from many researchers (Gardner 1996). This approach was first developed by van Oss, Chaudhury, and Good, as they tried to relate the surface tension components more closely with their chemical nature, and is also known as the vOCG method (Van Oss *et al.* 1988, 1990). Instead of

the polar component (hydrogen bond component) being described as  $\gamma^p$ , it was described as  $\gamma^{AB}$ , where  $AB$  refers to acid-base interactions. The non-polar (dispersion) term was described as  $\gamma^d$ ; this was changed to  $\gamma^{LW}$ , where  $LW$  describes all London-van der Waals forces. Thus, the surface free energy could be described as  $\gamma = \gamma^{LW} + \gamma^{AB}$ . As the polar term was redefined to take into account the acid-base interactions, the component  $\gamma^{AB}$  is a combination of contributions from electron donors ( $\gamma^-$ ) and electron acceptors ( $\gamma^+$ ). The sum of the acid-base components can then be redefined as  $\gamma^{AB} = 2\sqrt{\gamma^+\gamma^-}$ . The interfacial tension between the solid and liquid interface can then be defined by:

$$\gamma_{SL} = \gamma_S + \gamma_L - 2\sqrt{\gamma_S^{LW}\gamma_L^{LW}} - 2\sqrt{\gamma_S^+\gamma_L^-} - 2\sqrt{\gamma_S^-\gamma_L^+} \quad (3)$$

Combining this equation with Young's equation gives:

$$\gamma_L(1 + \cos\theta) = 2\sqrt{\gamma_S^{LW}\gamma_L^{LW}} + 2\sqrt{\gamma_S^+\gamma_L^-} + 2\sqrt{\gamma_S^-\gamma_L^+} \quad (4)$$

As there are now three terms relating to the solid surface, at least three known liquids are used for contact angle measurements, two of which must be polar liquids. The acid-base values of test liquids used according to vOCG have been listed in Table 1.

In the Young's equation, the contact angle means the equilibrium contact angle; however, the equilibrium contact angle on wood surfaces is difficult to directly acquire because of the chemical heterogeneity and surface roughness of wood, the fast absorption of the test liquids, and also the measuring condition. Meijer *et al.* (2000) and Wolkenhauer *et al.* (2007) noted that the thermodynamic equilibrium conditions assumed by Young's equation were not fulfilled with the wood surfaces. With respect to this, obtained results should be regarded with caution in their absolute value, but it should be noted that the objective of this study is to demonstrate the machined of woods surfaces with differently machined processes, so this approach seems to be suitable. Different methods for the determination of equilibrium contact angle that can be used to calculate the surface free energy of wood have been presented (Cao *et al.* 2005; Gindl *et al.* 2004; Jennings *et al.* 2006; Liptakova and Kudela 1994). In this study, the relative equilibrium contact angle (which is the intercept value of the regress line of contact angle values over time, the value at  $t = 0$  was taken to simulate the value of the equilibrium contact angle) was utilized to calculate the surface free energy of the wood samples, because many authors had indicated that the contact angle obtained by this method could evaluate the surface free energy of wood material successfully (Cao *et al.* 2005; Cao and Kamdem 2007; Maldas and Kamdem 1998; Mamiński *et al.* 2009; Nzokou and Kamdem 2004).

### Dynamic Wettability of Adhesives on Wood Surfaces

When the adhesive drop was placed on the wood surface, the contact angle was formed and decayed with increasing time due to the porosity and anisotropy of wood. Shi and Gardner (2001) proposed a wetting model (S-D model) (Shi and Gardner 2001) that has been most commonly used to evaluate the dynamic wetting process (Tang *et al.* 2012, Wei *et al.* 2012, Xu *et al.* 2010) among several decay models (Halliday *et al.* 1997; Liptakova and Kudela 1994; Nussbaum 1999; Topala and Dumitrascu 2007).

The equation of the S-D wetting model can be expressed as follows,

$$\theta = \frac{\theta_i \times \theta_e}{\theta_i + (\theta_e - \theta_i) \exp \left[ K \left( \frac{\theta_e}{\theta_e - \theta_i} \right) t \right]} \quad (5)$$

where  $\theta_i$  represents the initial (instantaneous) contact angle,  $\theta_e$  is the equilibrium contact angle,  $\theta$  represents the contact angle at a certain time,  $t$  represents wetting time, and  $K$  is a constant referring to the intrinsic relative contact angle decrease rate. The higher the value of  $K$  is, the faster the rate of adhesive penetration and spreading is. To obtain a  $K$  value for the adhesive and machined wood system, a nonlinear curve-fitting method can be used to fit the empirical data in Eq. 1.

It should be noted that the equilibrium contact angle  $\theta_e$  is a relative equilibrium contact angle because the ideal equilibrium state of adhesive on wood surface is difficult to achieve. However, the viscosity of PF adhesives were higher than the test liquids (*i.e.* distilled water, formamide, and diiodomethane), the change of contact angle as a function of time was slight when the time was increased, and the relative equilibrium contact angle can be obtained.

## RESULTS AND DISCUSSION

### Contact Angle

**Table 3.** Contact Angles of Different Machined Wood Samples

Sample		$\theta$ (degrees)		
		Water	Formamide	Diiodomethane
Planed	Sapwood	47.83(2.87)	20.89(0.94)	22.09(5.79)
	Heartwood	48.08(5.72)	26.87(0.86)	33.83(4.8)
Sawn	Sapwood	48.04(4.75)	33.18(2.8)	27.32(2.39)
	Heartwood	46.34(4.23)	26.81(4.06)	27.07(0.68)
Rotary	Loose side	104.18(6.91)	82.71(4.03)	46.92(3.6)
	Tight side	127.91(4.62)	95.65(2.92)	45.62(1.53)

Standard deviations shown in parentheses

The different machined processes affected surface wettability, as determined by contact angle measurements. The contact angles of test liquids acquired from using the linear regression method are shown in Table 3. For the wood surfaces machined by planing and sawing, no significant difference was observed in contact angle measurements, indicating that the effect of machined processes (planed and sawn) on contact angle were not remarkable. The contact angles of water on heartwood and sapwood were almost the same (between 46.34° to 48.08°), which may be because they have the same main chemical components of poplar wood (Gardner *et al.* 1991). The changes of contact angle for formamide and diiodomethane on the wood surface were also not significant, and it has been demonstrated that formamide is a strong hydrogen bonding liquid, which radically reduces the interfacial free energy at the liquid–solid

interface through acid-base interactions (Stehr *et al.* 2001); therefore, the contact angle was much smaller than that of water. Diiodomethane is an apolar liquid with low surface tension, so the contact angles were smaller than those of water. Compared with the planed and sawn wood samples, the contact angles of test liquids were highest on the rotary wood samples. The high contact angles of rotary wood may be caused by the different preparation technology of rotary wood samples; the extractives may have migrated from the interior to the exterior surface during the cooking and drying process. It is known that wood contains various extractives (Santoni and Pizzo 2011), such as terpenes, resins, phenolic compounds, triglycerides, fatty acids, and so on, and most of these are relatively hydrophobic. The frictional heat generated by rotary machining can be expected to cause these materials to migrate to the surface and smear over the surface of the wood, and a hydrophobic wood surface can be caused. The tight side and loose side also had different behaviors of wettability (Vázquez *et al.* 2003) because the wood surface was more dense on the tight side than on the loose side (Monni *et al.* 2007). As is shown in Table 1, the standard deviations of the contact angles were small; therefore, it could be concluded that the calculation method for acquiring the contact angle values is suitable.

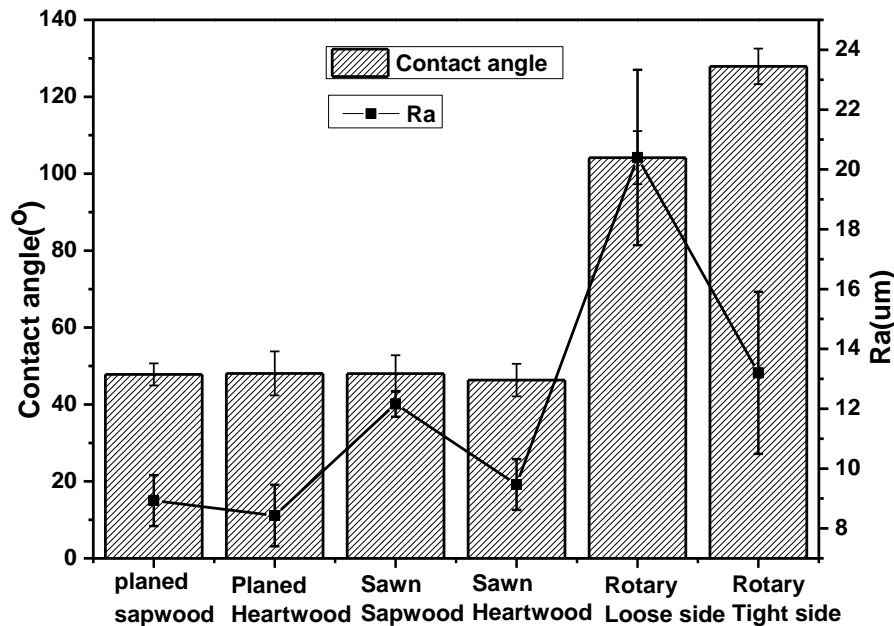
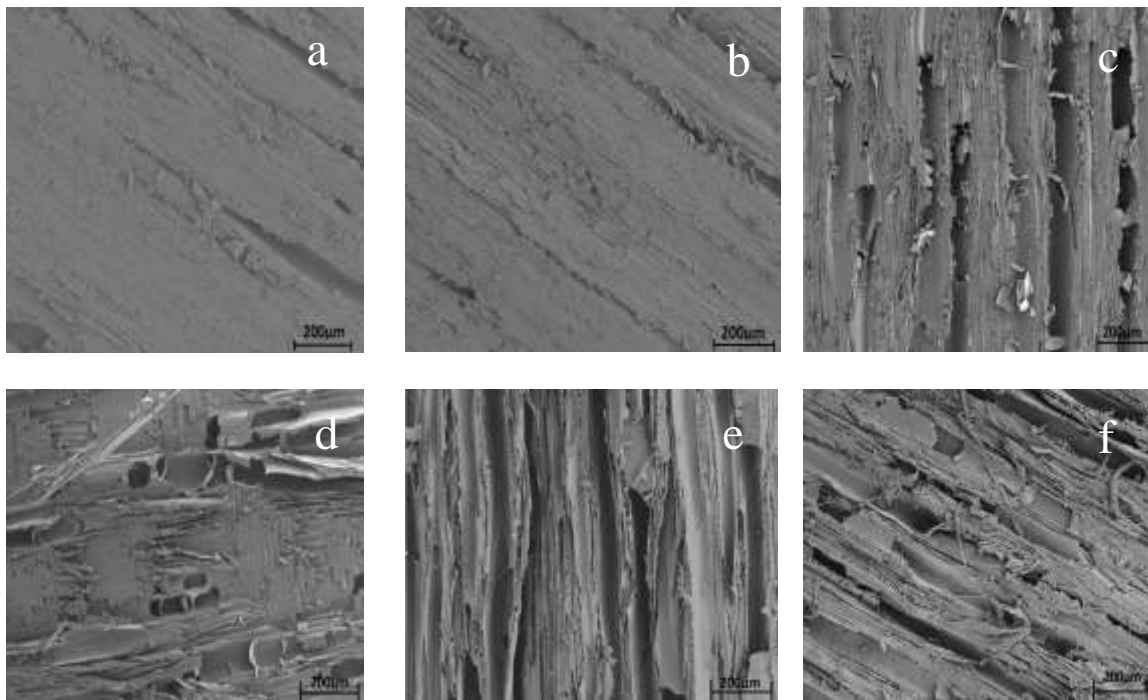


Fig. 1. Contact angles and surface roughness of different machine-processed samples

Surface roughness is an important property in terms of surface quality, particularly in finishing treatments (Buyuksari *et al.* 2011). The effects of surface roughness parameters (Ra) on the contact angles of water are shown in Fig. 1, and SEM micrographs of the different machined samples are shown in Fig. 2. As shown in Figs. 1 and 2, the rotary wood samples produced the most damaged and roughened surface structure, and were found to be much rougher than those of planed or sawn wood samples, especially on the loose side (Ra, 20.4 µm), which was 2.5 times rougher than that of the planed heartwood (Ra, 8.4 µm). The planed wood samples had the smoothest surface. It can be clearly seen from Fig. 2 that the roughness of planed wood samples were the smoothest compared with others, with few cell wall fibrillations on the surface. For sawn wood, a certain amount of vessels were destroyed and exposed on the surface

and the sawn wood had an intermediate level of fibrillation. The rotary tight side with less lathe checks was smoother than the loose side.

It was difficult to find a relationship between the change in contact angle and the surface roughness parameter. The tight side was much smoother than the loose side, but the contact angles were higher than those on the loose side. Compared with surface roughness, the effect of machined processes on contact angle of water was more significant than that of roughness, and many other factors also influenced the contact angle on difference machined wood such as heterogeneity, penetration, and absorption (de Moura and Hernandez 2006).



**Fig. 2.** a–f SEM micrographs of the different machined wood samples (a. planed sapwood, b. planed heartwood, c. sawn sapwood, d. sawn heartwood, e. rotary loose side, f. rotary tight side)

### Surface Energy Components

The total surface free energy of wood and the dispersion (referring to London dispersion forces) and polar (referring mainly to hydrogen bonding) components were calculated using the OWRK method with the reference liquids of water and diiodomethane, as presented in Fig. 3. Results showed that when the surface free energy of wood was investigated, there was no significant distinction of surface free energy of wood by planing and sawing, as indicated by the contact angle data; also, the surface free energy of the heartwood and sapwood were similar. The total surface free energy and its components of rotary wood samples were lower than those of planed or sawn wood samples.

For all of the wood investigated (except the rotary wood), the total surface free energy ranged from  $60 \text{ mJ/m}^2$  to  $70 \text{ mJ/m}^2$ , which was higher than the data given in the literature; many authors have found that the surface free energy of wood ranges from  $40 \text{ mJ/m}^2$  to  $60 \text{ mJ/m}^2$  (Gardner 1996; Gindl and Tschegg 2002; Little *et al.* 2013). This may be caused by two reasons: the acquired method of contact angle used to calculate the surface free energy and differences in used reference liquids.

Despite the apparent differences, the data were suitable enough to evaluate the differences and trends of wood surface free energy. From Fig. 3, it could also be concluded that the polar component of heartwood was higher than that of sapwood, but not remarkably so.

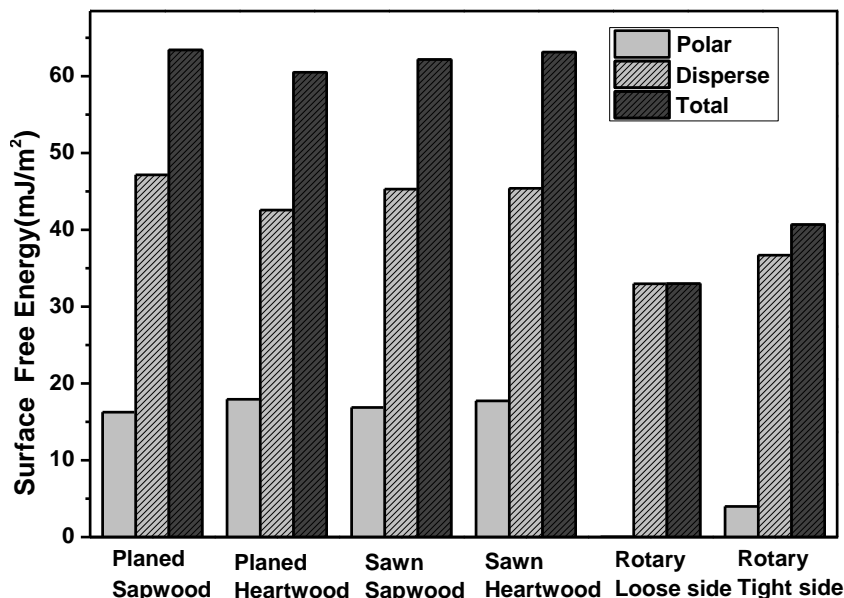


Fig. 3. Surface free energy of different machined samples calculated by the OWRK method

The total surface free energy, polar components, and dispersion component of rotary wood samples were all much lower than those of planed or sawn wood samples, and the polar component decreased significantly, especially on the loose side (only 0.01 mJ/m<sup>2</sup>). The lower surface free energy may have caused the higher initial contact angle. Many authors have indicated that the percentage of carbon on wood surface increases and oxygen percentage decreases with time, and the aging of a wood surface causes a decrease in the polar character of the wood surface and an increase in its hydrophobic character (Gardner *et al.* 1991, Gindl *et al.* 2004, Sernek *et al.* 2004).

The vOCG method provides for greater accuracy and more information than the OWRK method (Gardner 1996; Wålinder and Gardner 2002). The reference liquids of surface free energy calculations by the vOCG method using liquid parameters from van Oss were water, diiodomethane, and formamide. Table 4 shows that the calculated total surface free energy of machined wood were all lower than the total calculated by the OWRK method. The surface free energy ranged from 37.67 mJ/m<sup>2</sup> to 56.27 mJ/m<sup>2</sup> and the AB component and acid component of heartwood were higher than those of sapwood because the oxidation of extractives increased the acidity of the heartwood (Gindl *et al.* 2004).

No significant laws were found for the total surface free energy, LW component, and base component between the heartwood and sapwood. The surface free energy of rotary wood species calculated by the vOCG method using liquid parameters from van Oss *et al.* (1990) was lower than those for planed and sawn wood.

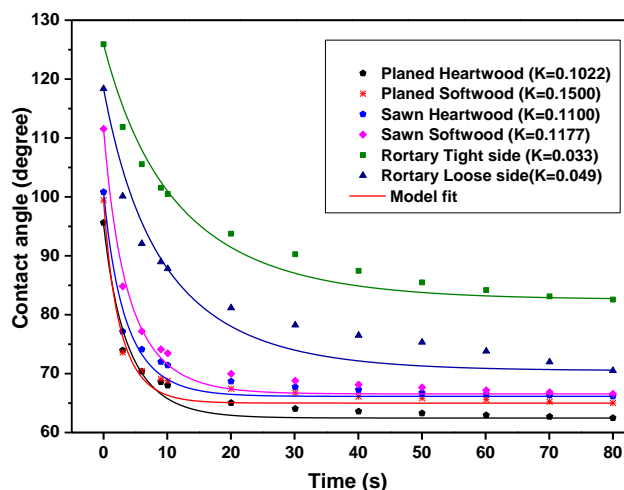
**Table 4.** Surface Free Energy of Different Machined Samples Obtained by the vOCG Method

Samples		$\gamma_s$	Surface Energy Components (mJ/m <sup>2</sup> )			
			$\gamma_s^{LW}$	$\gamma_s^{AB}$	$\gamma_s^+$	$\gamma_s^-$
Planed	Sapwood	56.27	47.14	9.13	0.93	22.42
	Heartwood	53.02	42.56	10.48	1.13	24.29
Sawn	Sapwood	50.76	45.29	5.50	0.27	27.97
	Heartwood	53.62	45.39	8.26	0.64	26.64
Rotary	Loose side	37.67	35.97	1.67	0.932	0.745
	Tight side	40.63	36.69	3.94	2.408	1.61

It is known that surface free energy calculated by the vOCG method using the vOCG reference liquids parameters often exaggerates the basicity (de Meijer *et al.* 2000; Gardner 1996; Wålinder 2002), and for machined wood other than the rotary wood, the basicity was much higher than the acidity. The surface free energy of machined wood species obtained using the liquid parameters given by Della Volpe and Siboni could effectively balance the relationship between the acid component and base component (Volpe and Siboni 1997; Wålinder 2002).

### Dynamic Wettability

Figure 4 shows the experimental data and the model fit line of the contact angle as a function of time for the different machined wood surfaces and adhesive A3. As shown in this figure, the contact angle of the adhesive decreased quickly during the initial 10 s of the wetting process, after which the contact angle slowly stabilized and reached a relative equilibrium state (Shi and Gardner 2001). During the initial stage, the contact angle decreased more rapidly on the planed and sawn wood surface (in the range of 0 to 20 s) than on the rotary wood surface (about 0 to 40 s). Also, the rotary wood surfaces showed higher equilibrium contact angles than the planed and sawn wood.

**Fig. 4.** Contact angle changes as a function of time for adhesive on machined wood surfaces

The K-values of adhesives on different machined surfaces, the asymptotic standard errors (SE), and the coefficients of determination ( $R^2$ ), all calculated by the software Origin 8.0 and the Marquardt-Levenberg algorithm, as well as the initial and

equilibrium contact angles, are all shown in Table 5. The regression equation had a high fitting degree: the coefficient of determination ( $R^2$ ) values were more than 95% for all of the wood surfaces examined, and the asymptotic standard errors (SE) were no more than 12% of the K-values. In this study, the wetting model could be used to accurately describe the adhesives wetting process on the different machined wood surfaces. The K-values in the model could be used to quantify the penetration and spreading rate of the adhesives and wood surfaces.

As shown in Table 5, for all of the wood samples, the initial and equilibrium contact angles increased as the viscosity of adhesives increased; the decrease percent and K-values also decreased for the planed and sawn samples, except with adhesive A2 on planed sapwood. The wettability of wood samples reduced with the increased viscosity of adhesives, consistent with the literature (Gavrilovic-Grmusca *et al.* 2012; Monni *et al.* 2007). Furthermore, the changes in surface tension of the three adhesives were not significant (from 66.87 mJ/m<sup>2</sup> to 68.23 mJ/m<sup>2</sup>, as shown in Table 1); therefore, the differences in contact angle were caused mainly by the change in viscosity.

**Table 5.** Contact Angles and K-values on Different Wood Surfaces with Different Adhesives

Species	Adhesives	Contact Angles			K-values		
		$\theta_i$ (degree)	$\theta_e$ (degree)	Percent Decrease (%)	K(1/s)	SE(1/s)	R2
Planed Sapwood	A1	87.53	49.06	47.7	0.120	0.012	0.960
	A2	99.43	65.00	34.6	0.150	0.0107	0.970
	A3	124.40	78.43	36.5	0.095	0.0045	0.990
Planed Heartwood	A1	86.06	45.00	43.9	0.178	0.017	0.969
	A2	95.64	62.47	34.7	0.102	0.0097	0.967
	A3	110.42	76.54	30.7	0.074	0.0063	0.970
Sawn Sapwood	A1	86.41	48.42	43.9	0.124	0.0088	0.979
	A2	111.56	66.56	40.3	0.118	0.0078	0.984
	A3	112.45	75.57	32.7	0.098	0.0094	0.968
Sawn Heartwood	A1	95.35	52.64	44.7	0.121	0.019	0.966
	A2	100.83	66.14	34.4	0.110	0.011	0.966
	A3	119.18	80.35	32.9	0.099	0.0068	0.985
Rotary Loose Side	A1	113.90	69.40	39.1	0.051	0.005	0.951
	A2	118.36	70.74	40.2	0.049	0.0043	0.950
	A3	128.90	98.60	23.5	0.022	0.0015	0.978
Rotary Tight Side	A1	121.30	82.09	32.4	0.027	0.0022	0.963
	A2	125.91	82.56	34.4	0.033	0.0024	0.977
	A3	133.25	103.82	22.1	0.026	0.0030	0.951

The change in the initial angle, equilibrium angle, K-value, and percent decrease for the heartwood and sapwood were all insignificant because the chemical components were almost the same, which was consistent with the difference between the contact angle of water and surface free energy. Shi *et al.* also observed that the effect of wood location (sapwood and heartwood) on adhesive wetting behavior is apparently insignificant (Shi and Gardner 2001).

The rotary wood samples had the highest initial and equilibrium contact angles, and the lowest K-value compared with others. The surface area of rotary wood samples was larger than that of planed wood or sawn wood, as shown in Fig. 2. The surfaces on

which the contact angles were measured were not freshly prepared before measuring, and this could be the cause of the difference; the aging might be the main reason the penetration decreased. As can be seen, contact angles decreased more rapidly on the loose side than the tight side when the viscosity of adhesives was low, and the existence of lathe checks and the horizontal flow on the loose side surface was predominantly responsible for the decrease of the contact angle (Vázquez *et al.* 2003). On the tight side, the change in K-value was not remarkable because of the slower penetration of adhesives.

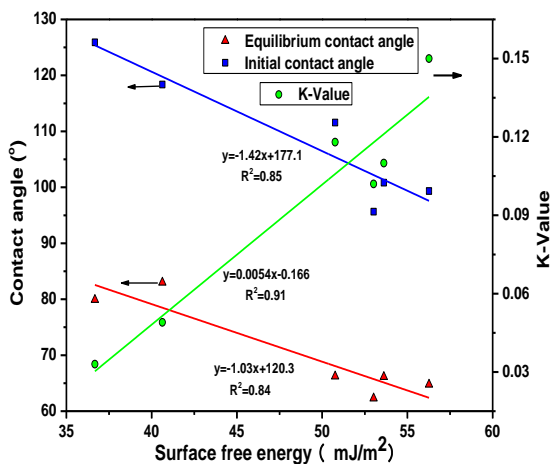


**Fig. 5.** The relationship between the initial contact angle, equilibrium contact angle, K-value, and surface free energy calculated by the OWRK method

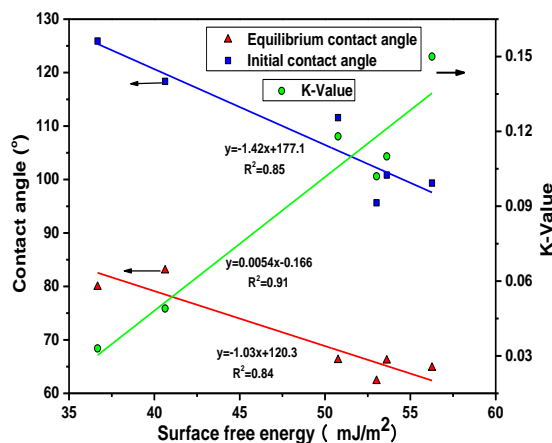


**Fig. 6.** The relationship between the initial contact angle, equilibrium contact angle, K-value, and surface free energy calculated by the vOCG method

Surface free energy is a significant characteristic that allows for the evaluation of interfacial interactions. The planed and sawn wood revealed similar total surface free energy values, which were significantly higher than the surface free energy found for rotary wood samples. The PF adhesive A3 was taken as an example for investigating the relationship between the contact angles, penetration, and surface free energy. Figures 5 and 6 show the initial contact angle, equilibrium contact angle, and K-values as a function of surface free energy. As expected, the contact angles decreased with increasing surface free energy, while the K-value increased.

The strengths of the relationships ( $R^2$ ) between the equilibrium contact angle and surface free energy calculated by the OWRK method (0.93) were greater than those calculated by the vOCG method (0.84); however, the agreements ( $R^2$ ) between the initial contact angle, K-value, and surface free energy calculated by the vOCG method (0.85 and 0.91, respectively) were better than those calculated by the OWRK method (only 0.81 and 0.61). From this relationship, it could be concluded that the effect of interaction between the methylol groups of PF adhesive and hydroxyls of wood surface samples on the contact angles was remarkable and that the initial contact angle, equilibrium contact angle, and K-value could be predicted by surface free energy; however, more data is needed to prove this.

In summary, it may be suggested that the structure anisotropy of differently machined wood surface samples affects surface free energy and penetration significantly, and rotary-processed wood in particular possesses rather different wettability compared with the other samples.

## CONCLUSIONS

1. The contact angles of the reference liquids on rotary wood samples were greater than those on planed or sawn wood samples; the effect of surface roughness on contact angle was insignificant compared with surface structure morphology.
2. The total surface free energy was almost the same for the planed wood and sawn wood. The surface free energy of rotary wood samples calculated by the OWRK method and vOCG methods was lower than that of planed or sawn wood.
3. The initial and equilibrium contact angles increased as the viscosity of PF adhesives increased for all wood samples; the contact angle of rotary wood samples was greater than those of planed and sawn wood, while penetration was lower, and the wettability of the loose side was higher than that of the tight side.
4. The rotary-processed wood possessed significantly different surface free energy and dynamic wettability compared with the other samples.
5. Contact angles decreased with increasing surface free energy, whereas the K-value increased.

## ACKNOWLEDGMENTS

This research was supported by the Fundamental Research Funds for the Central Universities (NO. TD2011-12) and the National Natural Science Foundation of China (Project 31000268/C160302).

## REFERENCES CITED

- Baldan, A. (2012). "Adhesion phenomena in bonded joints," *International Journal of Adhesion and Adhesives* 38(7), 95-116.
- Buyuksari, U., Akbulut, T., Guler, C., and As, N. (2011). "Wettability and surface roughness of natural and plantation-grown narrow-leaved ash (*Fraxinus angustifolia* Vahl.) wood," *BioResources* 6(4), 4721-4730.
- Cao, J.-Z., Li, L.-D., and Liu, Z. (2005). "Effect of ACQ-D treatment on the surface free energy of Chinese fir (*Cunninghamia lanceolata*)," *Forestry Studies in China* 7(4), 29-34.
- Cao, J., and Kamdem, P. D. (2007). "Surface energy of preservative-treated southern yellow pine (*Pinus* spp.) by contact angle measurement," *Frontiers of Forestry in China* 2(1), 99-103.
- de Meijer, M., Haemers, S., Cobben, W., and Militz, H. (2000). "Surface energy determinations of wood: Comparison of methods and wood species," *Langmuir* 16(24), 9352-9359.
- de Moura, L. F., and Hernandez, R. E. (2006). "Evaluation of varnish coating performance for three surfacing methods on sugar maple wood," *Forest Products Journal* 56(11-12), 130-136.
- Elbez, G. (1978) "Study of wettability of wood," *Holzforschung* 32(3), 82-92.

- Gardner, D. J. (1996). "Application of the Lifshitz-van der Waals acid-base approach to determine wood surface tension components," *Wood and Fiber Science* 28(4), 422-428.
- Gardner, D. J., Generalla, N. C., Gunnells, D. W., and Wolcott, M. P. (1991). "Dynamic wettability of wood," *Langmuir* 7(11), 2498-2502.
- Gavrilovic-Grmusa, I., Dunky, M., Miljkovic, J., and Djiporovic-Momcilovic, M. (2012). "Influence of the viscosity of UF resins on the radial and tangential penetration into poplar wood and on the shear strength of adhesive joints," *Holzforschung* 66(7), 849-856.
- Gindl, M., Reiterer, A., Sinn, G., and Stanzl-Tschegg, S.E. (2004). "Effects of surface ageing on wettability, surface chemistry, and adhesion of wood," *Holz als Roh- und Werkstoff* 62(4), 273-280.
- Gindl, M., Sinn, G., Gindl, W., Reiterer, A., and Tschegg, S. (2001a). "A comparison of different methods to calculate the surface free energy of wood using contact angle measurements," *Colloids and Surfaces A: Physicochemical and Engineering Aspects* 181(1-3), 279-287.
- Gindl, M., Sinn, G., Reiterer, A., and Tschegg, S. (2001b). "Wood surface energy and time dependence of wettability: A comparison of different wood surfaces using an acid-base approach," *Holzforschung* 55(4), 433-440.
- Gindl, M., and Tschegg, S. (2002). "Significance of the acidity of wood to the surface free energy components of different wood species," *Langmuir* 18(8), 3209-3212.
- Gray, V.R. (1962). "The wettability of wood," *Forest Prod. J.* 12(9), 452-461.
- Halliday, D. R., Resnick, R., and Walker, J. (1997). *Fundamentals of Physics*, John Wiley & Sons, Inc, New York.
- Han, S.-G., Huang, R.-Z., Zhou, Z.-B., and Zhang, Y. (2009). "Dynamic wettability of pre-compressed poplar," *Journal of Nanjing Forestry University* 33(6), 11-14.
- Hse, C. Y. (1972). "Wettability of southern pine veneer by phenol formaldehyde wood adhesives," *Forest Prod. J.* 22(1), 51-56.
- Hua, Y.-K., and Jin, J.-W. (2006) "Status and development of the southern type poplar processing industry in Jiangsu province," *China Wood Industry* 20(2), 72-75.
- Huang, X., Kocaefe, D., Kocaefe, Y., Boluk, Y., and Pichette, A. (2012). "Changes in wettability of heat-treated wood due to artificial weathering," *Wood Science and Technology* 46(6), 1215-1237.
- Jennings, J. D., Zink-Sharp, A., Frazier, C. E., and Kamke, F. A. (2006). "Properties of compression-densified wood, Part II: Surface energy," *Journal of Adhesion Science and Technology* 20(4), 335-344.
- Jennings, J. D., Zink-Sharp, A., Kamke, F. A., and Frazier, C. E. (2005). "Properties of compression densified wood. Part 1: bond performance," *Journal of Adhesion Science and Technology* 19(13-14), 1249-1261.
- Liptakova, E., and Kudela, J. (1994). "Analysis of the wood-wetting process," *Holzforschung* 48(2), 139-144.
- Little, N. S., McConnell, T. E., Irby, N. E., Shi, S. Q., and Riggins, J. J. (2013). "Surface free energy of blue-stained southern pine sapwood from bark beetle-attacked trees," *Wood and Fiber Science* 45(2), 206-214.
- Maldas, D. C., and Kamdem, D. P. (1998). "Surface tension and wettability of CCA-treated red maple," *Wood and Fiber Science* 30(4), 368-373.

- Mamiński, M.Ł., Mierzejewska, K., Borysiuk, P., Parzuchowski, P., and Boruszewski, P. (2009). "Surface properties of octadecanol-grafted pine veneers," *International Journal of Adhesion and Adhesives* 29(8), 781-784.
- Mohammed-Ziegler, I., Oszlanczi, A., Somfai, B., Horvolgyi, Z., Paszli, I., Holmgren, A., and Forsling, W. (2004). "Surface free energy of natural and surface-modified tropical and European wood species," *Journal of Adhesion Science and Technology* 18(6), 687-713.
- Monni, J., Alvila, L., and Pakkanen, T. T. (2007). "Structural and physical changes in phenol-formaldehyde resol resin, as a function of the degree of condensation of the resol solution," *Industrial & Engineering Chemistry Research* 46(21), 6916-6924.
- Nussbaum, R. M. (1999). "Natural surface inactivation of Scots pine and Norway spruce evaluated by contact angle measurements," *Holz als Roh- und Werkstoff* 57(6), 419-424.
- Nzokou, P., and Kamdem, D. P. (2004). "Influence of wood extractives on moisture sorption and wettability of red oak (*Quercus rubra*), black cherry (*Prunus serotina*), and red pine (*Pinus resinosa*)," *Wood and Fiber Science* 36(4), 483-492.
- Owens, D. K., and Wendt, R. C. (1969). "Estimation of the surface free energy of polymers," *Journal of Applied Polymer Science* 13(8), 1741-1747.
- Rathke, J., and Sinn, G. (2013). "Evaluating the wettability of MUF resins and pMDI on two different OSB raw materials," *European Journal of Wood and Wood Products* 71(3), 335-342.
- Santoni, I., and Pizzo, B. (2011). "Effect of surface conditions related to machining and air exposure on wettability of different Mediterranean wood species," *International Journal of Adhesion and Adhesives* 31(7), 743-753.
- Sernek, M., Kamke, F. A., and Glasser, W. G. (2004). "Comparative analysis of inactivated wood surfaces," *Holzforschung* 58(1), 22-31.
- Shi, S. Q., and Gardner, D. J. (2001). "Dynamic adhesive wettability of wood," *Wood and Fiber Science* 33(1), 58-68.
- Stehr, M., Gardner, D.J., and Wålinder, M. E. P. (2001). "Dynamic wettability of different machined wood surfaces," *The Journal of Adhesion* 76(3), 185-200.
- Tang, L., Zhang, R., Zhou, X., Pan, M., Chen, M., Yang, X., Zhou, P., and Chen, Z. (2012). "Dynamic adhesive wettability of poplar veneer with cold oxygen plasma treatment," *BioResources* 7(3), 3327-3339.
- Topala, I., and Dumitrascu, N. (2007). "Dynamics of the wetting process on dielectric barrier discharge (DBD)-treated wood surfaces," *Journal of Adhesion Science and Technology* 21(11), 1089-1096.
- Vázquez, G., Galiñanes, C., Freire, M.S., Antorrena, G., and González-Alvarez, J. (2011). "Estudio del mojado y caracterización superficial por microscopía de barrido laser confocal de chapas de madera obtenidas por desenrollo," *Maderas. Ciencia y Tecnología* 13(2), 183-192.
- Vázquez, G., González-Álvarez, J., López-Suevos, F., and Antorrena, G. (2003). "Effect of veneer side wettability on bonding quality of *Eucalyptus globulus* plywoods prepared using a tannin-phenol-formaldehyde adhesive," *Bioresource Technology* 87(3), 349-353.
- van Oss, C. J., Giese, R. F., and Good, R. J. (1990). "Reevaluation of the surface tension components and parameters of polyacetylene from contact angles of liquids," *Langmuir* 6(11), 1711-1713.

- van Oss, C. J., Good, R. J., and Chaudhury, M. K. (1988). "Additive and nonadditive surface tension components and the interpretation of contact angles," *Langmuir* 4(4), 884-891.
- Volpe, C. D., and Siboni, S. (1997). "Some reflections on acid–base solid surface free energy theories," *J. Colloid Interface Sci.* 195(1), 121-136.
- Wålinder, M. E. P. (2002). "Study of Lewis acid-base properties of wood by contact angle analysis," *Holzforschung* 56(4), 363-371.
- Wålinder, M. E. P., and Gardner, D. J. (2002). "Acid–base characterization of wood and selected thermoplastics," *Journal of Adhesion Science and Technology* 16(12), 1625-1649.
- Wei, S. Y., Shi, J. Y., Gu, J. Y., Wang, D., and Zhang, Y. H. (2012). "Dynamic wettability of wood surface modified by acidic dyestuff and fixing agent," *Applied Surface Science* 258(6), 1995-1999.
- Wolkenhauer, A., Avramidis, G., Cai, Y., Militz, H., and Viol, W. (2007). "Investigation of wood and timber surface modification by dielectric barrier discharge at atmospheric pressure," *Plasma Processes and Polymers* 4(S1), S470-S474.
- Xu, H.-N., Shen, Q.-Y., Ouyang, X.-K., and Yang, L.-Y. (2010). "Wetting of soy protein adhesives modified by urea on wood surfaces," *European Journal of Wood and Wood Products* 70(1-3), 11-16.

Article submitted: January 13, 2014; Peer review completed: March 16, 2014; Revised version received: March 20, 2014; Further revisions received and accepted: April 7, 2014; Published: April 10, 2014.